

Message Type 28

Todd Walter, Andrew Hansen, and Per Enge
Stanford University

ABSTRACT

The Wide Area Augmentations System (WAAS) and similar Satellite Based Augmentation Systems (SBASs) broadcast differential Global Positioning System (GPS) corrections and confidences. From this information a user can more accurately determine position. Even more importantly, the users can determine the confidence they have in that position solution. The format of the messages containing these corrections is described in the WAAS Minimum Operational Performance Standards (MOPS) [1]. A new message type is described that contains a relative clock and ephemeris covariance matrix for individual satellites. From this matrix users can reconstruct their location specific error bound rather than applying the largest bound in the service volume. By transmitting this information to the user, we can achieve two benefits: improved availability within the service volume and improved integrity in the region outside.

Message Type 28 contains matrices for two satellites per message, and each message is broadcast at the same rate as the long-term corrections (Message Type 25). Message Type 28 is in the process of being incorporated into the WAAS and has been presented to RTCA and to the International Civil Aviation Organization (ICAO) for inclusion in the MOPS and the international Standards And Recommended Procedures (SARPS). Two issues have been identified with its implementation. Complexity is added to the system in generating and monitoring the contents of the message. Additionally, the discretization error incurred when fitting the message into the limited bandwidth of the correction channel reduces some of the provided benefit. Nevertheless, we will show that application of this message achieves its goals. Clock and ephemeris errors are more accurately bounded outside the service volume, and projected confidence factors inside the service volume are reduced by more than 25%.

INTRODUCTION

The Wide Area Augmentation System (WAAS) and other similar Satellite Based Augmentation Systems (SBASs) broadcast differential GPS corrections and integrity information valid over continental scales. This data includes corrections for the broadcast satellite ephemeris and clock errors, corrections for ionospheric delay, and confidence limits on these corrections. Unfortunately, this vast quantity of information must be squeezed into a 250 bit per second (bps) data channel. The mechanism for broadcasting this data is described in detail in the Minimum Operational Performance Standards (MOPS) [1] [2]. An important component of this correction stream is a scalar confidence bound for the clock and ephemeris corrections per satellite. This confidence bound, termed User Differential Range Error (UDRE), is broadcast in the form of a variance, σ_{UDRE}^2 .

Since the UDRE is a single scalar value, it must protect all users within the service volume. As such, each UDRE must take on the largest projected value observable in that region, although the majority of the users would otherwise apply a significantly smaller value. In addition, outside the service volume, integrity would not be guaranteed. Here, the projected error could grow larger than within the service volume. A single UDRE, applicable everywhere in the footprint of the geostationary satellite, would preclude high levels of performance in the service volume.

Another message, Message Type 27, has been envisioned for application to the out of service zone problem. However, it is not a very elegant solution as it was originally created to mitigate atmospheric events. Message Type 27 is primarily static in time, geographically fixed, and applies to all satellites equally within its specified regions. Therefore, it can only mimic the true degradation in a conservative fashion. Additionally, it does not offer availability benefits within the service volume.

A new message, Message Type 28, broadcasts the full information set from which the UDRE was derived. Because less information is lost in the transmission channel, we greatly reduce the disadvantages of the scalar UDRE. Now the full 4-dimensional clock-ephemeris covariance matrix can be broadcast to the users. From this matrix users can reconstruct their location specific error bound rather than applying the largest bound in the service volume. For certain users this may reduce the effect of UDRE by factors of three or more. All users will see some availability benefit as no single location experiences the worst projected error bound on all satellites simultaneously, as is assumed without Message Type 28. Since these matrices are sent per satellite, they are dynamic and not geographically fixed. The true error bound can now be accurately modeled both inside and outside the service volume.

MOPS DESCRIPTION OF MESSAGE TYPE 28

Message Type 28 may be broadcast to provide the relative covariance matrix for clock and ephemeris errors. This is an expansion on the information contained in the UDRE in that it specifies the correction confidence as a function of user location. A single scalar UDRE bounds the error for the worst-case user in the service volume. Users within the service volume may have smaller bounds than the broadcast UDRE, while users outside the service volume will have larger uncertainties. Message Type 28 provides increased availability inside the service volume and increased integrity outside.

The covariance matrix is a function of satellite location, reference station observational geometry, and reference station measurement confidence. Consequently it is a slowly changing function of time. Each covariance matrix need only be updated on the same order as the long-term corrections. Each message is capable of containing relative covariance matrices for two satellites. The covariance matrices will be scaled by the broadcast UDRE. This maintains the real-time six-second update of integrity and scales the matrix to keep it within a reasonable dynamic range.

Cholesky factorization [3] is used to reliably compress the information in the covariance matrix, \mathbf{C} . The Cholesky factor is an upper triangular matrix, \mathbf{R} . This information can be used to reconstruct the full covariance matrix as $\mathbf{R}^T \mathbf{R} = \mathbf{C}$, where the superscript T denotes the matrix transpose. This factorization guarantees that the received covariance matrix remains positive definite despite quantization errors. Because \mathbf{R} is upper triangular, it contains only 10 non-zero elements. These 10 elements

are broadcast in half of Message Type 28. The elements of \mathbf{R} can be written as

$$\mathbf{R} = \begin{bmatrix} R_{1,1} & R_{1,2} & R_{1,3} & R_{1,4} \\ 0 & R_{2,2} & R_{2,3} & R_{2,4} \\ 0 & 0 & R_{3,3} & R_{3,4} \\ 0 & 0 & 0 & R_{4,4} \end{bmatrix} \quad (1)$$

What is broadcast in the message is actually a scaled version of \mathbf{R} . This broadcast matrix, \mathbf{E} , and a scale exponent are transmitted in Message Type 28 (see Table 1). The scale factor is given by

$$\text{scale factor} = 2^{\text{scale exponent} - 5} \quad (2)$$

The Cholesky factorization matrix is given by

$$\mathbf{R} = \text{scale factor} \times \mathbf{E} \quad (3)$$

and the relative clock ephemeris correction covariance is reconstructed by

$$\mathbf{C} = \mathbf{R}^T \cdot \mathbf{R} \quad (4)$$

The relative covariance matrix is used to modify the broadcast UDRE values as a function of user position. The change to the UDRE value is specified by

$$\delta UDRE \equiv \sqrt{\mathbf{l}^T \cdot \mathbf{C} \cdot \mathbf{l}} + \varepsilon_C \quad (5)$$

where \mathbf{l} is the four dimensional line of site vector from the user position (\mathbf{r}_{user}) to the satellite position (\mathbf{R}_{SV}) in the WGS-84 coordinate frame given by

$$\mathbf{l} \equiv \begin{bmatrix} \mathbf{r}_{user} - \mathbf{R}_{SV} \\ |\mathbf{r}_{user} - \mathbf{R}_{SV}| \\ 1 \end{bmatrix} \quad (6)$$

The additional term, ε_C , is to compensate for the errors introduced by quantization. Its value is connected to the scale factor broadcast in the message by

$$\varepsilon_C = \text{scale factor} \times C_{\text{covariance}} \quad (7)$$

Originally it was envisioned that $C_{\text{covariance}}$ would be hard-coded to a value of one half. Later it was determined that this would be insufficient and that $C_{\text{covariance}}$ should be broadcast in Message Type 10 so that it could be updated. The final MOPS format has not been decided at the time of this writing. For the remainder of the paper we will assume that $C_{\text{covariance}} = 1/2$.

Parameter	No. of Bits (Note 1)	Effective Range (Note 1)	Units
IODP	2	0 to 3	discrete
PRN Mask No. (Note 2)	6	0 to 51	—
Scale exponent. (Note 3)	3	0 to 7	discrete
$E_{1,1}$	9	0 to 511	discrete
$E_{2,2}$	9	0 to 511	discrete
$E_{3,3}$	9	0 to 511	discrete
$E_{4,4}$	9	0 to 511	discrete
$E_{1,2}$	10	± 512	discrete
$E_{1,3}$	10	± 512	discrete
$E_{1,4}$	10	± 512	discrete
$E_{2,3}$	10	± 512	discrete
$E_{2,4}$	10	± 512	discrete
$E_{3,4}$	10	± 512	discrete
PRN Mask No. (Note 2)	6	0 to 51	---
Scale exponent. (Note 3)	3	0 to 7	discrete
$E_{1,1}$	9	0 to 511	discrete
$E_{2,2}$	9	0 to 511	discrete
$E_{3,3}$	9	0 to 511	discrete
$E_{4,4}$	9	0 to 511	discrete
$E_{1,2}$	10	± 512	discrete
$E_{1,3}$	10	± 512	discrete
$E_{1,4}$	10	± 512	discrete
$E_{2,3}$	10	± 512	discrete
$E_{2,4}$	10	± 512	discrete
$E_{3,4}$	10	± 512	discrete

Table 1. Message Type 28 Contents.

Notes:

- 1) All signed values are coded as two's complement, with the sign bit occupying the MSB. The effective range is smaller than indicated, as the maximum positive value is actually constrained to be one value less (the indicated value minus the resolution).
- 2) Mask sequence. The count of 1's in mask from the first position in mask to the position representing the subject satellite. If set to 0, no satellite is represented and the remainder of the message should be ignored.
- 3) A Single scaling factor multiplies each of the **E** elements. It is given by $2^{(\text{scale exponent} - 5)}$. Thus the overall scale factor for each element ranges from 2^{-5} to 2^2 by discrete powers of 2.

Note that the line of sight defined in (6) or its negative would be acceptable because (5) only depends on the square of **l**. The sign can be defined either way. Also **l** is

not critically sensitive to either \mathbf{R}_{SV} or \mathbf{r}_{user} . \mathbf{R}_{SV} can be either the broadcast satellite position or the SBAS corrected position with negligible differences. Similarly, \mathbf{r}_{user} can be the uncorrected position or a previous position.

The $\delta UDRE$ in (5) replaces the value in (A-46) of [1]. Thus, a service provider could use Type 27 or Type 28, but not both.

Table 1 presents the contents of Message Type 28 representing the Cholesky factor of the clock-ephemeris covariance matrix for two WAAS satellites. The covariance matrices are accompanied by the IODP associated with the PRN mask. Refer to Section A.4.4.2 for the application of IODP.

The PRN Mask No. is the sequence number of the bits set in the 210 bit mask (that is, between 1 and 51). As opposed to data in Message Types 2 - 5, the data in this Type 28 message does not have to appear in sequence. The IODP of the message must agree with the IODP associated with the PRN mask in Message Type 1.

Figure 1 also presents the contents of the Type 28 message. There is a single IODP that applies to both matrices broadcast. The remainder of the 212 data bits is divided in two and each half contains identically formatted information for one satellite. Thus, Message Type 28 is capable of broadcasting clock-ephemeris messages for up to two satellites.

GENERATION OF MESSAGE

The information to broadcast in Message Type 28 comes from the observations of the ground based reference stations. Much like the user is able to determine position using multiple satellites, a service provider can determine satellite position using known reference station locations. The distribution of the observing reference stations and their measurement quality can be used to determine the covariance matrix for projecting confidence to specific user locations.

We can define an observation matrix, **G**, whose rows can be related to the line of sight vector (6) except the

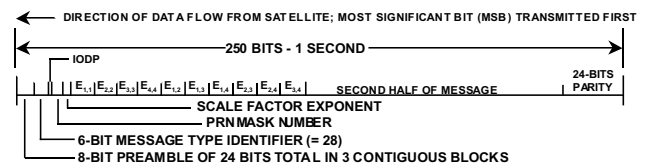


Figure 1. Type 28 Clock-Ephemeris Covariance Matrix

reference station position, $\mathbf{r}_{RS,i}$, would take the place of \mathbf{r}_{user} .

$$\mathbf{G}_i = \begin{bmatrix} -l_{x,i} & -l_{y,i} & -l_{z,i} & -1 \end{bmatrix} = -\mathbf{I}_i \quad (8)$$

The subscript i for the i^{th} row of the matrix refers to the i^{th} reference station. The observation matrix relates the difference between the broadcast satellite position and clock, and the true position and clock, $\Delta\mathbf{X}_{SV}$, to the resulting differences in pseudorange, $\Delta\mathbf{y}$,

$$\Delta\mathbf{y} = \mathbf{G} \cdot \Delta\mathbf{X}_{SV} + \boldsymbol{\epsilon} \quad (9)$$

where $\Delta\mathbf{X}_{SV}$ is the satellite position error vector augmented by clock error

$$\Delta\mathbf{X}_{SV} = \begin{bmatrix} X_{true} - X_{broadcast} \\ Y_{true} - Y_{broadcast} \\ Z_{true} - Z_{broadcast} \\ B_{true} - B_{broadcast} \end{bmatrix} \quad (10)$$

and $\boldsymbol{\epsilon}$ is the vector of observation errors.

The equation above can be inverted to find the snapshot estimate of satellite position and clock error

$$\Delta\mathbf{X}_{SV} = (\mathbf{G}^T \cdot \mathbf{W} \cdot \mathbf{G})^{-1} \cdot \mathbf{G}^T \cdot \mathbf{W} \cdot \Delta\mathbf{y} \quad (11)$$

The uncertainty in that snapshot estimate is described by the four by four dimensional clock and ephemeris covariance matrix, \mathbf{P} ,

$$\mathbf{P} \equiv (\mathbf{G}^T \cdot \mathbf{W} \cdot \mathbf{G})^{-1} \quad (12)$$

This matrix contains the information describing how the uncertainty in the estimate maps onto different lines of sight. It is the information in this matrix that we wish to convey in the combination of Message Type 28 and the UDRE.

The product of $\delta UDRE$ from Message Type 28 and the broadcast UDRE must overbound the user's projected clock and ephemeris correction uncertainty. Because the UDRE is broadcast every six seconds while MT28 is broadcast only every 120 seconds, MT28 should be viewed as providing the relative shape of the projections while the UDRE provides the absolute value. Note that one may be multiplied by an arbitrary constant and the other may be divided by that same constant without altering the end result. This leaves us flexibility in deciding how to normalize the covariance. To optimize availability we would like to normalize the covariance matrix so that the

UDRE falls in the densest region of quantized values. For backwards compatibility we would want to normalize at the largest projected value in the service volume. For convenience we may wish to normalize at the minimum projected value. We will proceed with the latter choice for this paper, although the user is protected for whichever option chosen. A search may be required to find the minimum value but it will likely be very near the weighted average of the reference station lines of sight. We will call the minimizing line of sight \mathbf{l}_{min} and the corresponding minimum projection P_{min}

$$P_{min} = \min_{\text{all } \mathbf{l}_{\text{elevation}} > 5^\circ} \mathbf{l} \cdot \mathbf{P} \cdot \mathbf{l} = \mathbf{l}_{min} \cdot \mathbf{P} \cdot \mathbf{l}_{min} \quad (13)$$

If we divide the \mathbf{P} we obtained from (12) by our normalization value, we have the quantity we wish to discretize and put into MT28

$$\mathbf{C}_{full} \equiv \frac{\mathbf{P}}{P_{min}} \quad (14)$$

The covariance matrix in (12) is based on a snapshot solution. Various methods have been proposed to lower the uncertainty in the error. Two of the most prominent schemes are the use of dynamical orbit information [4] and the use of *a priori* information [5]. Both provide similar benefits as far as yielding better conditioned matrices and allowing solutions to be obtained with fewer than four reference stations. Dynamical orbit estimation yields the highest accuracy, but require longer time intervals of data. The use of *a priori* information is far simpler but relies on the continued good performance of the broadcast error. Both have issues with regard to integrity and certification. Here we will investigate only the incorporation of *a priori* information.

We know from observations that the expected broadcast orbital accuracy is quite good. Jefferson and Bar-Sever found the accuracy to be better than a few meters [6]. The largest observed errors were around 60 m. This *a priori* information could be included in the position solution. The least squares fit seeks to minimize measurement residuals. The solution in (11) minimizes the cost function

$$\Delta\mathbf{y}^T \cdot \mathbf{W} \cdot \Delta\mathbf{y} \quad (15)$$

The inclusion of *a priori* information minimizes a different cost function

$$\Delta\mathbf{X}_{SV}^T \cdot \mathbf{P}_0^{-1} \cdot \Delta\mathbf{X}_{SV} + \Delta\mathbf{y}^T \cdot \mathbf{W} \cdot \Delta\mathbf{y} \quad (16)$$

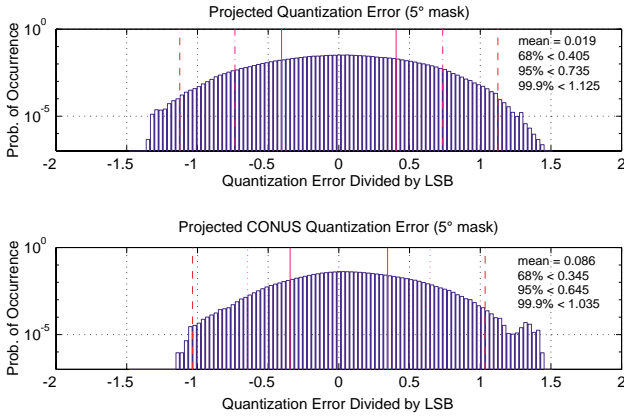


Figure 2. Histograms of projected discretization error normalized by the value of the scale factor (18). The scale factor is also the Least Significant Bit (LSB).

There is a balance between minimizing measurement residuals and offsetting the satellite from its expected location. The resulting covariance matrix is

$$\mathbf{P} = (\mathbf{P}_0^{-1} + \mathbf{G}^T \cdot \mathbf{W} \cdot \mathbf{G})^{-1} \quad (17)$$

In this paper we investigate two different *a priori* conditions. One is based on the historical observations of Jefferson et al. And the other is based on the limitations of the magnitudes of the corrections in the MOPS message format. The first conservatively describes nominal performance, but it may be difficult to demonstrate its integrity. The second provides less benefit but should be provably safe. For the historical *a priori* we conservatively set the diagonal elements of \mathbf{P}_0 to $(3 \text{ m})^2$, $(10 \text{ m})^2$, $(10 \text{ m})^2$, and infinite (no *a priori* claimed on the clock). This was in a radial, along-track, and cross-track frame. This matrix had to be rotated into the Earth centered earth fixed (ECEF) frame before application in (17). For the MOPS limited *a priori* we used the dynamic range of the corrections. Message Type 25 can support orbital errors as large as 128 meters for each of the X, Y, and Z directions. Message Types 2-5 and Type 25 combined can support a clock error of about 410 meters. Thus, the MOPS limited *a priori* is a diagonal matrix with $(128 \text{ m})^2$ for the first three elements and $(410 \text{ m})^2$ for the fourth. If the broadcast errors were really larger than the MOPS limit, this constraint would not be sufficient to override the measurements. It will be shown, however, that it is sufficient to improve quantization error.

QUANTIZATION ERROR

The limited number of bits in which the covariance matrix is broadcast results in non-negligible quantization error. The magnitude of this error is directly related to the scale factor. The larger the value of the Least Significant Bit

(LSB) is, the greater the possible error in the discretized version of the covariance matrix can be. If the discretized projection is smaller than the true projection, an integrity violation may result. The term ϵ_c is included to prevent such integrity violations. Unfortunately, as originally defined, this protection was not guaranteed. Although usually sufficient, certain geometries may lead to an underbounding greater than $\epsilon_c = \text{scale factor} \times 0.5$. Theoretically, the underbounding may be several times the magnitude of the least significant bit. However, a fairly extensive Monte Carlo exploration has found that the maximum underbounding is limited to 1.4 times the least significant bit. This limit was found to be independent of assumed noise profile, *a priori*, and normalization point.

Figure 2 shows histograms of projected discretized error divided by the scale factor. This is defined by

$$\frac{\sqrt{\mathbf{I}^T \cdot \mathbf{C} \cdot \mathbf{I}} - \sqrt{\mathbf{I}^T \cdot \mathbf{C}_{full} \cdot \mathbf{I}}}{2^{\text{scale exponent} - 5}} \quad (18)$$

where \mathbf{C} is the discretized version of the matrix (4) and \mathbf{C}_{full} (14) is the full floating point version. On average, this distribution is reasonably zero-mean gaussian with a sigma of roughly one third. However, specific cases will vary. For some matrices the errors will all be positive and for others primarily negative (see Figure 3). Fortunately, this is deterministic; once we have \mathbf{C}_{full} we can find \mathbf{C} and then determine the projection errors.

For integrity purposes it is the minimum projected discretization error in the service volume that is most important. This will result in the most significant underbounding. The UDRE must be large enough to

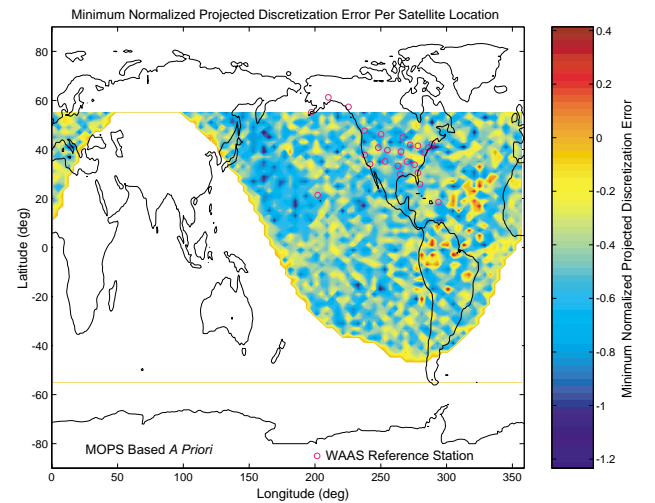


Figure 3. Minimum projected discretization error is shown as a function of satellite location. This simulation uses a presumed noise distribution and *a priori* information.

cover this error. Unfortunately the constraints on \mathbf{I} make finding this minimum difficult. There may be several local minima and the true global minima may be fairly narrow. This makes finding the true minimum a non-trivial task. Here again the *a priori* can help. Even the MOPS limit based *a priori* significantly smoothes the projection of \mathbf{C}_{full} compared to no *a priori*. This broadens the sharp local minima thus easing the effort of minimum finding.

The upper histogram of Figure 2 is for projections throughout the visibility region of the satellite. The lower histogram is for projections within the primary coverage area of the reference station network. For a WAAS simulation this would be the CONUS region. Notice that restricting projections to the service region offers a slight improvement but does not significantly change the distribution.

Figure 3 shows a map of the minimum projected discretization error as a function of satellite location. The *a priori* assumed here corresponds to the MOPS limit and certain noise profiles were assumed for the reference stations to generate the \mathbf{W} matrix. The specifics of the map are very sensitive to such parameters. The important point is the random nature of the distribution. Although there are some large-scale trends, the minimum projected error will vary quite rapidly with reference station geometry. It all depends on the errors in the discretized Cholesky factorization. Small changes in \mathbf{C}_{full} will change the magnitudes and signs of these quantization errors leading to large differences in the projected quantization error.

Figures 4 and 5 show distributions of scale factors for different conditions. The three cases in Figure 4 correspond to when \mathbf{C}_{full} is normalized to the minimum point as defined in (13) and (14). It is obvious that tightening the *a priori* lowers the scale factor exponent. Since each index lower cuts the least significant bit in half, the resulting quantization error difference is dramatic. The maximum index that can be broadcast is 2. Therefore if no *a priori* is used there will be geometries that do not fit within the dynamic range of Message Type 28. Use of the MOPS based *a priori* curtails these upper excursions and ensures that the matrix remains within the dynamic range. Using the historically based *a priori* leads to an even more significant decrease in quantization error.

Another parameter that affects dynamic range and least significant bit is the normalization point for \mathbf{C}_{full} . Figure 4 shows the histogram for when it is normalized at the minimum projected value, but it is possible to normalize this matrix at different points. If we followed a backward compatible notion of normalizing the matrix at the

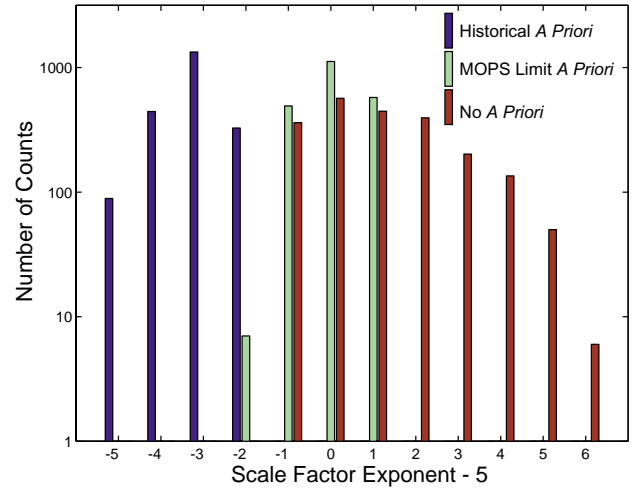


Figure 4. Histogram of scale factor exponents for different *a priori* values, when \mathbf{C}_{full} is normalized at the minimum point.

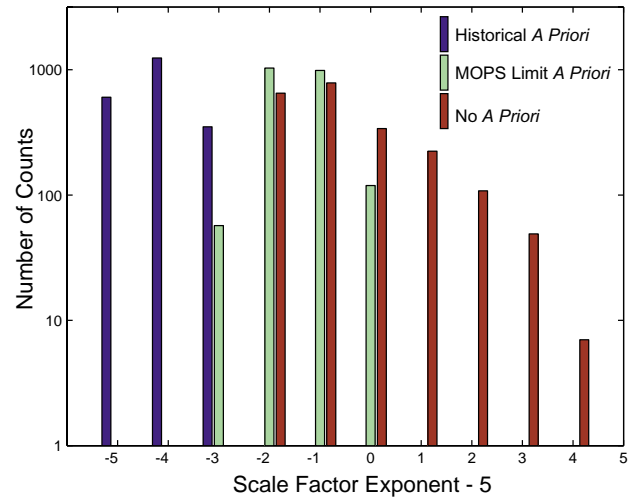


Figure 5. Histogram of scale factor exponents for different *a priori* values, when \mathbf{C}_{full} is normalized at the maximum point in CONUS.

maximum projected covariance within the service volume, we get the distributions shown in Figure 5. Note that these distributions are nearly one index lower than the preceding case. Thus, the quantization error is cut nearly in half for this normalization choice. Of course there are many factors influencing selection of normalization point and this choice will likely increase quantization error of the UDRE.

An interesting suggestion was made by Doug Tyler of Raytheon [7] to reduce the quantization error. He recognized that the fourth diagonal element of the \mathbf{R} matrix would always be 1 if the covariance matrix were normalized at the minimum. He suggested defining this term to be 1 and distributing its nine bits among the other nine elements. This would double their range and cut

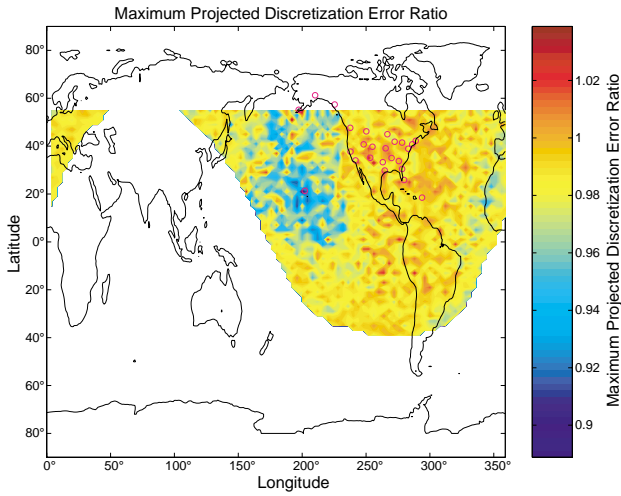


Figure 6. Maximum ratio of the full, normalized covariance matrix to $\delta UDRE$. The σ_{UDRE} at the satellite location can be multiplied by the specific value to gain availability (if less than 1) or to maintain integrity (if greater than 1).

quantization error in half. However, it would make normalizing at the minimum point mandatory. This may be undesirable in that it limits options for different service providers and may force a greater discretization penalty on the UDRE.

The quantization errors in Message Type 28 must be protected either by the ε_C term or by increasing the broadcast UDRE. The condition we must satisfy is

$$\sigma_{UDRE} \cdot \delta UDRE \geq \sqrt{\mathbf{I}^T \cdot \mathbf{P} \cdot \mathbf{I}} \quad (19)$$

everywhere in the service volume. Using the definition of $\delta UDRE$ from (5), and assuming we normalize at the minimum, we can place the condition on the broadcast UDRE as

$$\frac{\sigma_{UDRE}}{\sqrt{P_{\min}}} \geq \frac{\sqrt{\mathbf{I}^T \cdot \mathbf{C}_{full} \cdot \mathbf{I}}}{\sqrt{\mathbf{I}^T \cdot \mathbf{C} \cdot \mathbf{I} + \varepsilon_C}} \quad (20)$$

for all \mathbf{I} in the service volume. This can be satisfied by

$$\sigma_{UDRE} = \sqrt{P_{\min}} \max_{\mathbf{I} \text{ service volume}} \frac{\sqrt{\mathbf{I}^T \cdot \mathbf{C}_{full} \cdot \mathbf{I}}}{\sqrt{\mathbf{I}^T \cdot \mathbf{C} \cdot \mathbf{I} + \varepsilon_C}} \quad (21)$$

The maximum ratio in (21) is a much stronger function of assumed *a priori*, reference station geometry and noise profile than (18). Figure 6 shows the maximum ratio for the historically based *a priori* as a function of satellite location. For the particular choice of the ε_C term here,

$C_{\text{covariance}} = 1/2$, this ratio is less than one the majority of the time. Thus, σ_{UDRE} can be reduced to overcome discretization error and gain availability. However, some of the time σ_{UDRE} must be increased to maintain integrity.

APPLICATION OF MESSAGE

Let us consider an example. We will assume reference stations at the current WAAS placements, a satellite at 21°N, 204°W, and an assumed noise profile. For this example the observation matrix is

$$\mathbf{G} = \begin{bmatrix} 0.8521 & -0.4958 & -0.1679 & -1 \\ 0.8483 & -0.4943 & -0.1898 & -1 \\ 0.7686 & -0.5523 & -0.3227 & -1 \\ 0.8373 & -0.5190 & -0.1720 & -1 \\ 0.7913 & -0.5693 & -0.2229 & -1 \\ 0.8135 & -0.5487 & -0.1926 & -1 \end{bmatrix} \quad (22)$$

The weighting matrix has units of meters⁻² and is

$$\mathbf{W} = \text{diagonal} \begin{bmatrix} 2.8079 \\ 5.7812 \\ 6.7394 \\ 1.0842 \\ 0.1049 \\ 0.1883 \end{bmatrix} \quad (23)$$

From these we can form the product $\mathbf{G}^T \mathbf{W} \mathbf{G}$

$$\mathbf{G}^T \cdot \mathbf{W} \cdot \mathbf{G} = \begin{bmatrix} 11.1310 & -7.0740 & -3.2082 & -13.6209 \\ -7.0740 & -13.6209 & 2.1073 & 8.6979 \\ -3.2082 & 2.1073 & 1.0334 & 3.9895 \\ -13.6209 & 8.6979 & 3.9895 & 16.7059 \end{bmatrix} \quad (24)$$

To find the covariance matrix, we need to add (24) to the inverse of the *a priori* as described by (17). Here we used the historical based *a priori*. The covariance matrix is

$$\mathbf{P} = \begin{bmatrix} 65.9410 & 11.5212 & -37.4832 & 56.7169 \\ 11.5212 & 12.1237 & -6.7844 & 4.7016 \\ -37.4832 & -6.7844 & 31.2340 & -34.4881 \\ 56.7169 & 4.7016 & -34.4881 & 52.0914 \end{bmatrix} \quad (25)$$

which has units of meters². The minimum projected value of this matrix, P_{min} , is 0.0599 m². Figure 7 shows the projected covariance for all surface users with a viewing angle greater than 5°. Dividing (25) by P_{min} leads to the dimensionless \mathbf{C}_{full} .

$$\mathbf{C}_{full} = 10^3 \cdot \begin{bmatrix} 1.1016 & 0.1925 & -0.6262 & 0.9475 \\ 0.1925 & 0.2025 & -0.1133 & 0.0785 \\ -0.6262 & -0.1133 & 0.5218 & -0.5762 \\ 0.9475 & 0.0785 & -0.5762 & 0.8702 \end{bmatrix} \quad (26)$$

In order to fit this into Message Type 28 we need to take the Cholesky factorization

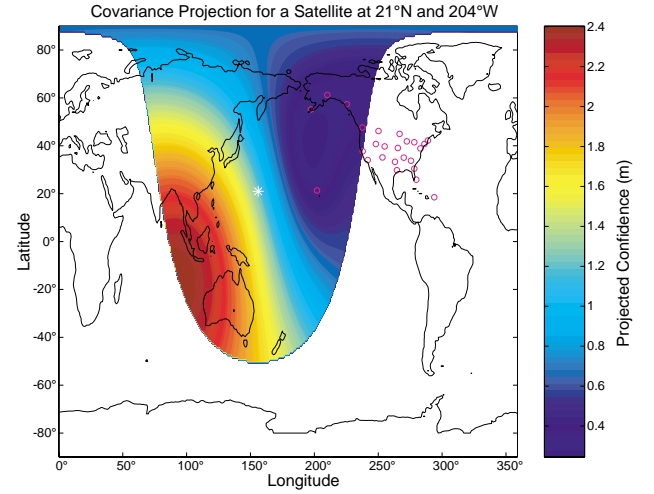


Figure 7. Projected user confidence from full covariance matrix (25).

$$\mathbf{R}_{full} = \begin{bmatrix} 33.1904 & 5.7990 & -18.8666 & 28.5476 \\ 0 & 12.9965 & -0.3025 & -6.6944 \\ 0 & 0 & 12.8745 & -3.0745 \\ 0 & 0 & 0 & 1.0000 \end{bmatrix} \quad (27)$$

This value must be discretized as described earlier. The smallest scale factor that will enable (27) to fit in the message constraints is 0.125. The resulting discretized version is given by

$$\mathbf{R} = \begin{bmatrix} 33.25 & 5.75 & -18.875 & 28.5 \\ 0 & 13 & -0.25 & -6.75 \\ 0 & 0 & 12.875 & -3.125 \\ 0 & 0 & 0 & 1 \end{bmatrix} \quad (28)$$

The broadcast matrix is then

$$\mathbf{E} = \begin{bmatrix} 266 & 46 & -151 & 228 \\ 0 & 104 & -2 & -54 \\ 0 & 0 & 103 & -25 \\ 0 & 0 & 0 & 8 \end{bmatrix} \quad (29)$$

The user can then reconstruct the bandwidth limited \mathbf{C} according to (4)

$$\mathbf{C} = 10^3 \cdot \begin{bmatrix} 1.1056 & 0.1912 & -0.6276 & 0.9476 \\ 0.1912 & 0.2021 & -0.1118 & 0.0761 \\ -0.6276 & -0.1118 & 0.5221 & -0.5765 \\ 0.9476 & 0.0761 & -0.5765 & 0.8686 \end{bmatrix} \quad (30)$$

which can be compared to (26). Figure 8 shows the projection of \mathbf{C} onto the user space. Note the similarities in shape to Figure 7. As expected the minimum projected

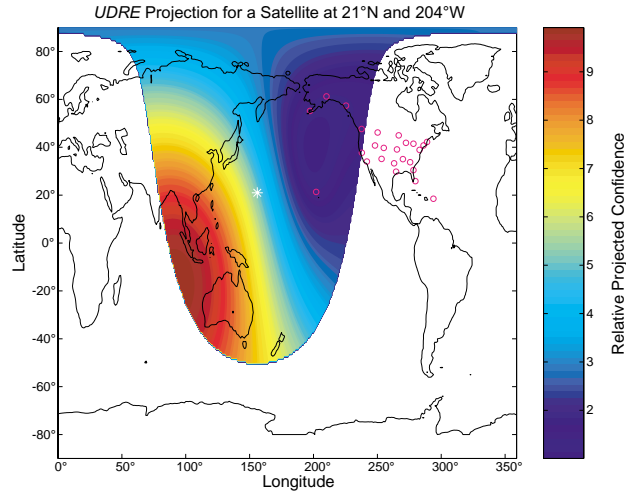


Figure 8. Projected user confidence according to the normalized discretized \mathbf{C} matrix (30).

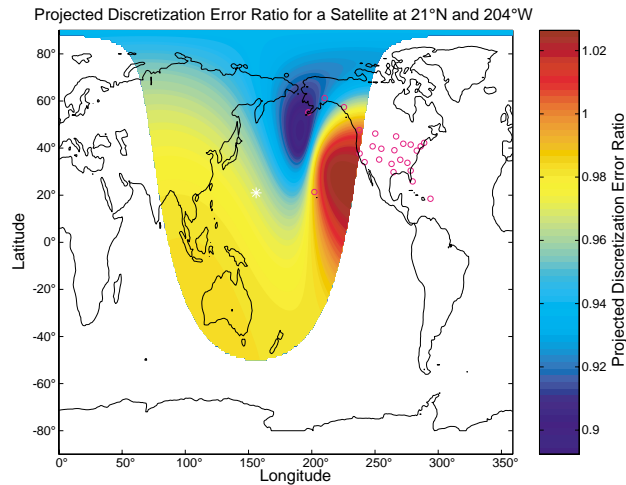


Figure 9. Projected ratio of the full bandwidth covariance divided by δ_{UDRE} as defined by (31). The UDRE will need to be scaled by this value.

value of this normalized matrix is 1. Figure 9 shows the projected discretization error ratio in the matrix \mathbf{C} defined by

$$\frac{\sqrt{\mathbf{I}^T \cdot \mathbf{C}_{full} \cdot \mathbf{I}}}{\sqrt{\mathbf{I}^T \cdot \mathbf{C} \cdot \mathbf{I} + \varepsilon_C}} \quad (31)$$

Here the maximum CONUS value is about 1.02. Therefore the quantization error in this matrix would need to be protected by increasing the σ_{UDRE} by about 2%. Thus, by following the requirements of (20) and (21), the broadcast σ_{UDRE} could be no smaller than 0.2496 m. Quantization of the σ_{UDRE} will require the transmitted value to be 0.3040 m.

AVAILABILITY IMPROVEMENT

One of the benefits of utilizing Message Type 28 is the potential for better availability. When not using Message Type 28, the service provider must broadcast the σ_{UDRE} that corresponds to the worst-case projection in the service volume. This is a pessimistic approximation. No location will correspond to the worst-case projection point for all satellites simultaneously. Therefore, by incorporating Message Type 28 a user should be able to lower some or all projected clock and ephemeris variances.

To investigate the magnitude of this effect we examined the projected $\delta UDRE$ from the message (5) relative to the maximum full bandwidth value in the service volume. To account for discretization error, this ratio was scaled by the maximum projected discretization ratio as in (21). This final value

$$\frac{\sqrt{\mathbf{I}^T \cdot \mathbf{C} \cdot \mathbf{I} + \varepsilon_C}}{\max_{\text{I service vol.}} \sqrt{\mathbf{I}^T \cdot \mathbf{C}_{full} \cdot \mathbf{I}}} \max_{\text{I service vol.}} \frac{\sqrt{\mathbf{I}^T \cdot \mathbf{C}_{full} \cdot \mathbf{I}}}{\sqrt{\mathbf{I}^T \cdot \mathbf{C} \cdot \mathbf{I} + \varepsilon_C}} \quad (32)$$

is the ratio of the projected confidence from use of Message Type 28 relative to not utilizing the message, for a particular line of sight.

Figure 10 shows histograms of this ratio (32) for two different conditions: a MOPS limit based *a priori* and a historically based *a priori*. As expected, smaller discretization errors lead to better performance. For the historically based *a priori*, this results in roughly a 32% reduction in the broadcast clock and ephemeris confidence. For the MOPS limited case, the reduction is still of order 26%. When quantization error can be further reduced, the lowering of confidence level can be improved to greater than 35%.

Notice that, for a small percentage of the projections, the quantization error is so large that utilizing Message Type 28 increases the projected confidence. In some cases this confidence is more than doubled. However, this only happens for the minority of cases and is more than offset by the number of times the confidence can be reduced. If this were of primary concern, note that these rare cases are determinable. A computationally intensive algorithm could determine when discretization error for a particular matrix would be worse than not utilizing Message Type 28. In those instances Message Type 28 could broadcast the identity matrix and σ_{UDRE} would correspond to the worst value in the service volume adjusted to remove the effects of ε_C . This would optimize for availability in the service volume, but may lead to a loss of integrity outside.

This improvement in the projected clock and ephemeris confidence cannot be translated into an availability improvement without assuming values for the other confidences. For the initial version of WAAS, the ionospheric error confidences are expected to be larger than the clock and ephemeris terms. This will reduce the availability benefit. However in the longer term, GPS will offer second and third civil frequencies that will allow users to directly estimate their own ionospheric error. This will result in dramatically lower confidences for these terms. When this occurs, the UDRE will be the dominant term and the reduction offered by Message Type 28 will be significant.

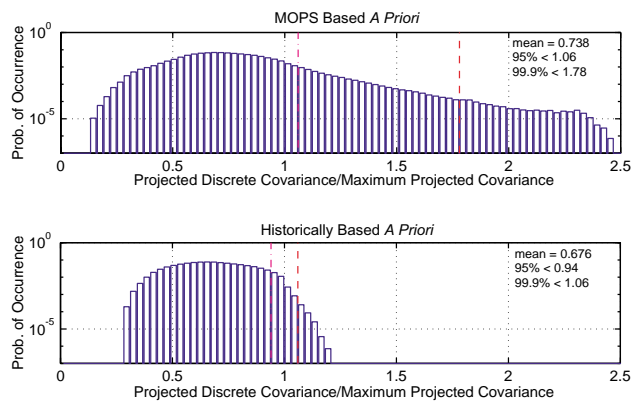


Figure 10. Histograms showing the reduction in projected confidence (32) when utilizing Message Type 28 for the MOPS limit based *a priori* and historically based *a priori*.

OUT OF SERVICE VOLUME PROTECTION

The other major benefit of Message Type 28 is that it can provide integrity for satellites everywhere in their viewing

area and not just in the service volume. Message Type 28 can be employed to provide en route integrity for oceanic routes far away from the reference network. As can be seen in Figure 8 the ratio of best to worst can exceed an order of magnitude. In this figure, a UDRE sufficient to protect the service volume can be more than 5 times too small for a user in Australia. However, when Message Type 28 is employed, the user gains protection both inside and outside of the service volume. Thus, Message Type 28 will increase the utility of SBASs in their intermediate regions [8] and will do so more efficiently than Message Type 27.

OLD BUT ACTIVE DATA

Messages broadcast by the service providers must be safe and accurate not only at the time of creation, but until they time out for the user as well. Thus, either the contents of Message Type 28 must be monitored and the UDREs adjusted as necessary, or the contents of the message must be made to be applicable over the lifetime of the message. Both have relative merits: monitoring the message in real-time is computationally intensive while pre-degrading the message at creation loses availability.

Monitoring in real-time would have its basis in Equation (21). The same equation would be used but now the denominator of the ratio would be based on already broadcast information and the other terms would be based on the current, yet to be broadcast covariance matrix. Another difficulty in real-time monitoring is that changes in viewing geometry can lead to sudden changes in the covariance matrix. This can cause sudden increases in UDRE and alarms. These alarms are caused by a lack of observability rather than a true error. Thus, there may be some instances when degrading the covariance matrix by the expected time-evolution of errors leads to better availability.

The degraded matrix would add *a posteriori* information to the covariance matrix (17). The new degraded matrix, \mathbf{P}_{deg} , would be of form

$$\mathbf{P}_{\text{deg}}(t) = \mathbf{P} + \mathbf{P}_{\text{err}}(t) \quad (33)$$

where \mathbf{P} is the undegraded matrix at time of creation (17), and $\mathbf{P}_{\text{err}}(t)$ describes the time evolution of the error terms. In the radial, along-track, and cross-track frame, $\mathbf{P}_{\text{err}}(t)$ will have form

$$\mathbf{P}_{\text{err}}(t) = \begin{bmatrix} \sigma_{\text{radial}}^2(t) & 0 & 0 & 0 \\ 0 & \sigma_{\text{along}}^2(t) & 0 & 0 \\ 0 & 0 & \sigma_{\text{cross}}^2(t) & 0 \\ 0 & 0 & 0 & \sigma_{\text{clock}}^2(t) \end{bmatrix} \quad (34)$$

Over the lifespan of the message the individual terms could be represented by simple polynomial expressions, $\sigma_{\text{radial}}(t)$, $\sigma_{\text{along}}(t)$, and $\sigma_{\text{cross}}(t)$ could be described as linear functions of time and $\sigma_{\text{clock}}(t)$ would be a quadratic function. This would properly describe the errors if all of the information were sent to the user at the same time. Unfortunately the ephemeris correction, clock correction, and covariance matrix span several messages with different update rates. In addition, some of these error terms are already present in the MOPS (Section A.4.5.1). For example, the clock correction is broadcast every six seconds, resetting this component of the error term to zero. Sections A.4.5.1.1 and A.4.5.1.2 of [1] already describe protection of the clock corrections. Section A.4.5.1.3 describes the protection of the ephemeris corrections.

In addition, the \mathbf{C} matrix in the message will be scaled by the UDRE. Therefore, we are only interested in how the orbital uncertainties affect the shape of \mathbf{C} . We can remove the clock term and leave the minimum point unchanged if we define a new matrix [9]

$$\mathbf{C}_{\text{err}}(t) = \frac{1}{P_{\text{min}}} \begin{bmatrix} [\mathbf{P}_{\text{eph}}]_{3 \times 3} & -[\mathbf{P}_{\text{eph}} \cdot \mathbf{I}_{\text{min}}]_{3 \times 1} \\ -[\mathbf{I}_{\text{min}}^T \cdot \mathbf{P}_{\text{eph}}]_{1 \times 3} & [\mathbf{I}_{\text{min}}^T \cdot \mathbf{P}_{\text{eph}} \cdot \mathbf{I}_{\text{min}}]_{1 \times 1} \end{bmatrix} \quad (35)$$

where P_{min} and \mathbf{I}_{min} correspond to the undegraded covariance matrix (13) and \mathbf{P}_{eph} is the upper left 3×3 portion of (34) rotated into the ECEF frame. This is the degradation term that must be added to \mathbf{C} , either before or after discretization.

CONCLUSIONS

Message Type 28 is a late, but important addition to the MOPS. This paper described its format as originally conceived. However, its final form has not yet been determined so one should check the latest version of the MOPS (DO-229C or later), which would take precedence over this paper.

Message Type 28 improves both availability inside the service volume and integrity outside the service volume. Its application is relatively simple for the user and optional for the service provider. Two issues remain with its use: it has non-negligible quantization error and it may be computationally costly for the service provider.

However, it has been shown that the reduction in projected confidence is still greater than any discretization penalty. Reductions between 25% and 35% were shown. While this may not lead to significant availability gains during early phases when other terms dominate, it will be very significant for end-state WAAS when this error source may be the limiting factor.

In addition, the service provider has plenty of leeway in its application. Different levels of benefit can be achieved depending on the complexity of implementation and tolerable computational load. Even for simplistic implementations there is significant reduction in projected confidence. In the future, as these problems become easier to address, more complex implementations will lead to greater improvements.

ACKNOWLEDGMENTS

The FAA GPS Product Team (AND-730) sponsored this work. We would also like to thank our colleagues participating in the WAAS Integrity Performance Panel (WIPP) for their guidance and numerous contributions. In particular we would like to thank Bruce DeCleene for both his guidance in determining the message format, and his championing this message both at RTCA and ICAO.

REFERENCES

[1] RTCA Special Committee 159 Working Group 2, "Minimum Operational Performance Standards for Global Positioning System / Wide Area Augmentation System Airborne Equipment," RTCA Document Number DO-229B, October 1999.

[2] T. Walter, "WAAS MOPS: Practical Examples," in Proceedings of the ION National Technical Meeting, San Diego, CA, January, 1999.

[3] G. Golub & C. van Loan, **Matrix Computations**, third edition, Johns Hopkins University Press Ltd., London, 1996.

[4] J. Ceva, B. Parkinson, W. Bertiger, R. Muellerschoen, and T. Yunck, "Incorporation of Orbital Dynamics to Improve Wide-Area Differential GPS," Global Positioning System Vol. VI, The Institute of Navigation, Alexandria, 1999.

[5] Y.J. Tsai, "Wide Area Differential Operation of the Global Positioning System: Ephemeris and Clock Algorithms," A Stanford University Ph.D. Dissertation, SUDAAR 716, August 1999.

[6] D.C. Jefferson and Y.E. Bar-Sever, "Accuracy and Consistency of Broadcast GPS Ephemeris Data," in Proceedings of ION-GPS-2000, Salt Lake City, UT, September, 2000.

[7] D. Tyler, Report to WIPP, September, 2000.

[8] J.P. Fenu, D. O'Laughlin, T.T. Hsiao, J. Reagan, R. Fuller, T. Walter, D. Dai, P. Enge, and J.D. Powell, "Interoperability of Satellite-Based Augmentation Systems," Global Positioning System Vol. VI, The Institute of Navigation, Alexandria, 1999.

[9] S.R. Peck, "A Method to Calculate MT28 OBAD," Report to WIPP, September, 2000